Optics Letters

# Fabrication and characterization of high-efficiency double-sided blazed x-ray optics

Istvan Mohacsi,[1,2,*] Ismo Vartiainen,[1] Manuel Guizar-Sicairos,[1] Petri Karvinen,[1] Vitaliy A. Guzenko,[1] Elisabeth Müller,[1] Cameron M. Kewish,[2] Andrea Somogyi,[2] and Christian David[1]

[1]Paul Scherrer Institut, Villigen PSI, 5232, Switzerland
[2]Synchrotron SOLEIL, L'Orme des Merisiers, Saint-Aubin, 91190, France
*Corresponding author: istvan.mohacsi@psi.ch

Received 11 November 2015; revised 7 December 2015; accepted 7 December 2015; posted 8 December 2015 (Doc. ID 253524); published 7 January 2016

**The focusing efficiency of conventional diffractive x-ray lenses is fundamentally limited due to their symmetric binary structures and the corresponding symmetry of their focusing and defocusing diffraction orders. Fresnel zone plates with asymmetric structure profiles can break this limitation; yet existing implementations compromise either on resolution, ease of use, or stability. We present a new way for the fabrication of such blazed lenses by patterning two complementary binary Fresnel zone plates on the front and back sides of the same membrane chip to provide a compact, inherently stable, single-chip device. The presented blazed double-sided zone plates with 200 nm smallest half-pitch provide up to 54.7% focusing efficiency at 6.2 keV, which is clearly beyond the value obtainable by their binary counterparts.** 

***OCIS codes:*** (050.1965) Diffractive lenses; (050.1970) Diffractive optics; (340.7460) X-ray microscopy; (220.4241) Nanostructure fabrication.

http://dx.doi.org/10.1364/OL.41.000281

Today's synchrotron radiation facilities offer a wide range of analytic methods, ranging from the extreme UV to the hard x-ray range [1,2]. Depending on the experimental scheme, x-ray optics not only provide high spatial resolution for microscopy but also allow for a better utilization of the available x-ray flux. Improved condenser efficiency allows us to deliver more photons to experiments, which can increase sensitivity in coherent diffractive imaging, trace element analysis, full-field x-ray microscopy, and time-resolved measurements or result in an overall reduction of measurement time. Diffractive x-ray optics, such as Fresnel zone-plate lenses [3], offer a compact optical setup with minimal demands on space and alignment, allowing great flexibility in their applications. However, they are often associated with low focusing efficiency. The latter originates from the fact that, while their resolution is comparable to their smallest zone width, the focusing efficiency of conventional Fresnel zone pates depends on their structure height [4]. The fabrication of both high-efficiency and high-resolution zone-plate optics for the multi-keV x-ray range thus requires high-aspect ratio metallic nanostructures. Even if manufacturing limitations regarding aspect ratio can be overcome, the focusing efficiency of binary zone plates is still fundamentally limited. As the binary structures diffract the same intensity to the focusing (positive) as to the defocusing (negative) diffraction orders, half of the diffracted intensity is always scattered into unwanted negative diffraction orders. This limitation can be surpassed by the use of blazed Fresnel zone plates, which have asymmetric structure profiles that break this symmetry in order to enhance the primary focusing order while suppressing others. As patterning techniques on the nanoscale are practically limited to discrete height levels, the ideal sawtooth-shaped structure profile needs to be approximated by staircase-shaped structures. Such multilevel zone plates have been reported in the literature using the patterning of multilevel structures [5] or by multilayer deposition [6]. However, practical issues concerning their working distance and resolution have hindered their practical use. As an alternative to pushing the limits of fabrication techniques, the stacking of zone plates [7–10] aims at improving the performance of existing Fresnel zone-plate lenses. By stacking two zone plates in each other's optical near field, they act as a single zone plate with added optical transmission profile. Hence by stacking a "coarse" binary zone plate with $\pi$ phase-shift and a double-density "fine" binary zone plate with $\pi/2$ phase shift, we effectively obtain a four-level, blazed profile identical to the one of multilevel zone plates [11,12]. This enables blazed zone-plate stacks to surpass the limitations of binary zone plates while only requiring binary structures made by well-established planar nanofabrication methods. Stacked zone plates were shown to provide superior efficiency compared with binary zone plates [12], but their everyday use requires a permanently fixed monolithic setup. Due to the potential gain in efficiency, significant efforts have been made to permanently glue together stacks of zone plates to provide a single-chip design [8,9]. However, the gluing process requires an online alignment of the two chips within an x-ray beam. Moreover, the glued stack is subject to drift during and even after the curing of the glue. As the two zone plates need to be aligned on the same optical axis, within one-third of the smallest zone width [13], even the slightest shift can compromise their optical performance. In this

Letter, we substitute mechanical alignment of stacked Fresnel zone plates with an aligned double-sided patterning process [10]. By patterning the two sides of the support membrane with the two zone plates for blazed stacking, we obtain the required four-level transmission in a monolithic optical element (Fig. 1).

We used the direct electron-beam writing of a Poly(methyl methacrylate) (PMMA) resist and subsequent electroplating of metallic nanostructures into the mold [14] to pattern our zone plates on the individual sides of our membranes. We prepared our zone plates on 250 nm thick and 2 mm × 2 mm sized rectangular silicon nitride membranes on 6 mm × 6 mm silicon frames. The substrates were coated with 25 nm gold and 5 nm chromium layers on both sides to serve as a conducting base for electroplating. We processed the two sides of the membrane separately, first the back side with the fine zone plate and then the front side with the coarse zone plate, as illustrated in Fig. 1. In the hard x-ray range and for moderate line widths as in this paper, it is irrelevant whether the fine or the coarse zone-plate side is facing toward the x-ray source as described in [15]. Regarding the sequence of fabrication, we found that a patterning of the dense zone plate on the back side of the membrane before patterning the coarse zone plate on the front side led to improved results. This is due to the fact that one of the most critical steps—the resist coating of the membrane back side—could be done as the first processing step at elevated spinning speed, leading to a more uniform resist layer.

The zone-plate patterns along with a set of alignment markers were exposed into the resist by 100 keV electron-beam lithography using a Vistec EBPG 5000+ES writer. In order to cover the entire process window and compensate for the forward scattering of the electron beam [16], each membrane was exposed with several zone plates with slightly different exposure doses. The patterned chips were developed in a mixture of isopropanol and water (7:3 by volume) cooled to 2°C for increased contrast [17]. The PMMA mold was filled with electroplated nickel using pulsed plating for uniform structure height [18]. The plating was stopped when the mold started to overplate. The patterning of the coarse zone plates on the front side involved a similar procedure, but the exposure of the zone-plate patterns was aligned to the first exposure by locating the previously exposed alignment markers through the membrane.

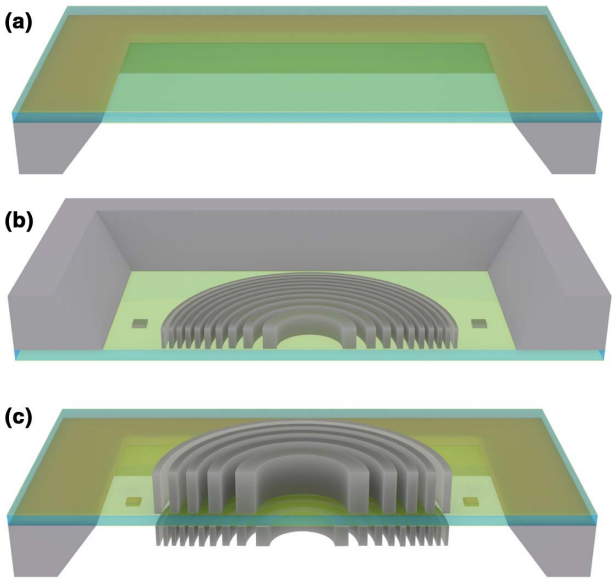


**Fig. 1.** Schematic fabrication process of the presented double-sided blazed Fresnel zone plates. (a) The membranes are coated with a chromium/gold/chromium plating base both on the front and the back side. (b) The first set of zone-plate structures giving a $\pi/2$ phase shift is patterned on the back side of the membrane together with a set of alignment markers (square patterns). (c) A set of zone-plate structures giving a $\pi$ phase shift are patterned on the front side of the membrane by a second exposure aligned to the markers through the membrane.

Using the above-described process, we produced several sets of double-sided blazed nickel zone plates with 100 μm diameter and 200 nm smallest half-pitch. The zone plates were characterized by scanning electron microscopy (SEM) (Fig. 2). Using high acceleration voltage and a backscattering electron detector, the larger structures of the other side can be detected; however, the smaller structures cannot be observed. Therefore, some double-sided blazed zone plates were sectioned using focused ion beam milling (FIB) (Fig. 3). In the FIB cross section, we can see the zone plates on both sides of the membrane. The dense structures on the back of the membrane are 1 μm high, while the coarse structures on the front side are 2.2 μm high below the overplating. This closely matches the targeted values required for $\pi$- and $\pi/2$-phase shifts at 6.2 keV photon energy.

A detailed characterization of double-sided blazed Fresnel zone-plate chips was performed at the cSAXS beamline of the Swiss Light Source, Paul Scherrer Institut, Switzerland. We measured the integral and spatially resolved diffraction efficiency at 6.2 keV photon energy (0.2 nm wavelength) and performed a ptychographic characterization of the lens transmission profile. For the efficiency measurements, we illuminated our zone plates through an aperture of equal diameter and the first diffraction order was selected by a 10 μm pinhole located in the focal plane. The average diffraction efficiency of the 93 tested zone plates was 45.4%, with diffraction efficiencies up to 54.7% (Fig. 4). These values clearly surpass the 36.8% fundamental limit of a binary nickel zone plate at this photon energy and are similar to the values demonstrated for blazed zone plates with micron-sized structures [5,6] or stacks that required a setup of mechanical actuators for alignment [12].

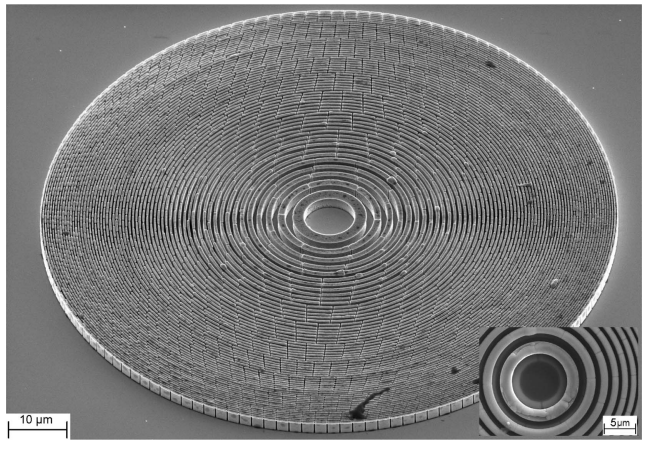


**Fig. 2.** A conventional SEM image of a blazed double-sided Fresnel zone plate shows only the front-side coarse zone plate. The inset shows the center of a zone plate using a backscattered-electron detector, revealing the central zones of the dense zone plate on the other side of the membrane.

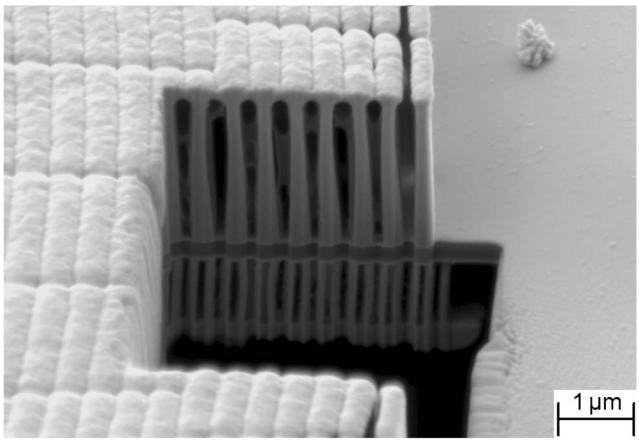


**Fig. 3.** FIB cross section of a blazed double-sided Fresnel zone plate imaged by SEM. The trapezoidal shape of the front-side zones is characteristic of the forward scattering of the electron beam in the thick resist layer.

The expanding diffraction cone of the first-order, zone-plate focus was recorded 7 m downstream of the focal plane on a Pilatus 2 M single-photon counting pixel detector [19]. The diffraction cone can be interpreted as a spatial map of the diffraction. Only three of our zone plates showed severe misalignment in the micron range, which manifested itself as moiré fringes in the diffraction cone.

As a sensitive measure for the alignment in the nanometer range, we determined the ratio of the ±1st diffraction orders. Therefore a zone plate with 45.3% overall efficiency was scanned with a 10 µm pencil beam and its diffraction patterns were recorded on the Pilatus 2 M detector. The recorded diffraction patterns consist of discrete spots, allowing one to map +1st and the −1st diffraction order simultaneously. The obtained map shows clear anticorrelation between +1st and the −1st diffraction orders (Fig. 5). The focusing +1st order dominates over the zone plate area focusing 48.4% of the incoming radiation into the primary focus. The defocusing −1st order with 10.0% overall efficiency is clearly suppressed. The −1st order only becomes substantial in two opposite regions near the edge of the zone plates. This indicates a misalignment in the corresponding direction. The ratio of +1st and −1st orders can be used as a measure for the local misalignment in radians, providing a map of the relative radial misalignment between the two sides. This suggests a 20–30 nm shift between the zone plates on the two sides of the sample.

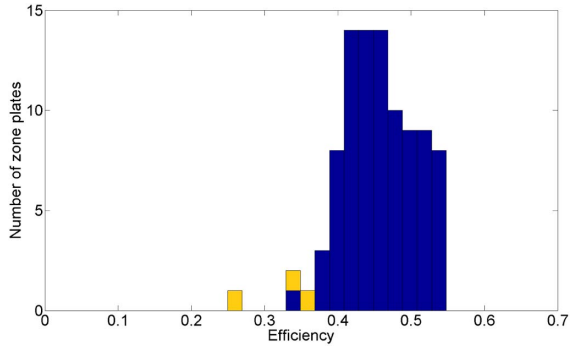


**Fig. 4.** Efficiency histogram of 93 double-sided blazed Fresnel zone plates. The best zone plate reaches 78% of its maximal possible value of 0.71. The spread in efficiency is caused by the different structure height and exposure parameters of our lenses. Three of the lowest efficiency lenses, marked in yellow, suffer from severe misalignment, but the majority of our lenses provide high-focusing efficiency, proving the reliability of the process.

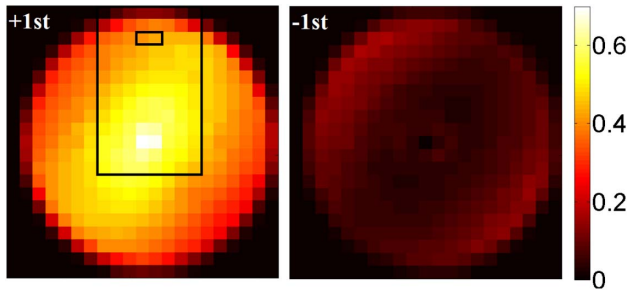


**Fig. 5.** Distribution of the focusing +1st and the defocusing −1st diffraction orders over a double-sided blazed zone plate with 45.3% overall efficiency. The +1st focusing order is clearly enhanced, while the defocusing −1st order is suppressed. Both efficiency maps show a clear anisotropy along the diagonal of the zone plate, which corresponds with a slight misalignment between the two sides. The black rectangles mark the position of the ptychographic mapping shown in Fig. 6.

In order to have a comprehensive measurement of the structure quality and alignment, we characterized the at-wavelength x-ray transmission profile using ptychography [20,21]. When using the lens as a sample, ptychography can directly measure its complex optical transmission function. A total of 36 µm × 65 µm area of the same lens was imaged with 300 nm step size. The total area was subdivided into subregions in order to avoid problems arising from slight changes in the illumination during the measurement [22]. The reconstruction was performed using the difference map algorithm [20] for 400 iterations and averaging the object over the final 100 iterations. The information behind the detector gaps was accounted in the reconstruction by an implementation of a shared reconstruction between multiple scans [22].

The reconstructed phase-shift profile (Fig. 6), clearly shows the four-step staircase profile both in the large central and the smaller outer zones. As ptychography produces quantitative results, the local diffraction efficiency of our zone plates can be obtained from the Fourier components of the retrieved complex optical transmission profile. This results in 50.4% diffraction efficiency even for the smallest structures (Fig. 6). This is significantly higher than the 43% that was measured by x-ray diffraction in that area of the zone plate. The mismatch can be explained by the fact that ptychography is not sensitive to the overall 5% absorption in the membrane. Additionally, the selected area did not contain any support structures as radial interruptions of the zones, which further explain the discrepancy between the two measurements. Since the zone plate is made of a single material with known optical constants, the phase profile provides us with an accurate height map of the structures. We obtained 2.1 µm for the coarse and 0.95 µm for the dense structures. This is close to the targeted values of 2.28 and 1.14 µm for $\pi$ and $\pi/2$ phase shift.

Double-sided patterning of Fresnel zone plates is a promising new technique for improving the efficiency of diffractive

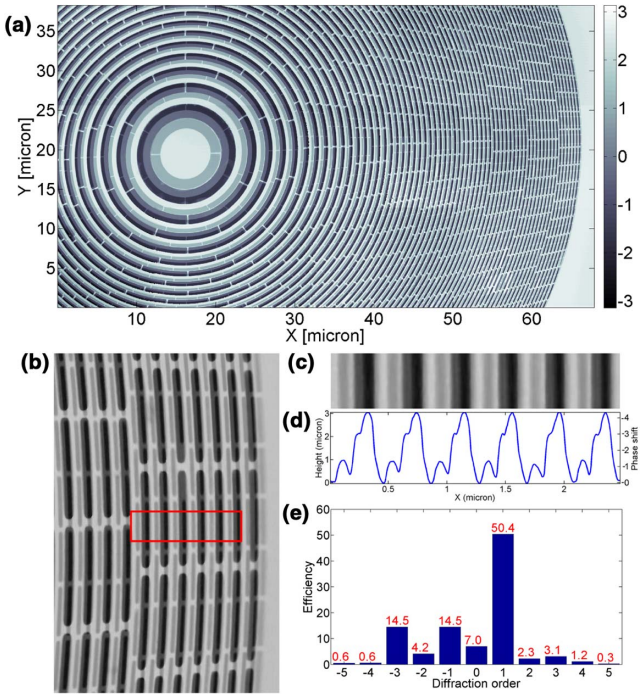


**Fig. 6.** (a) The phase profile of a double-sided blazed zone plate obtained by ptychographic imaging. The four-step transmission profile is clearly visible among the large central zones. (b) The magnified section shows the phase profile of the smallest zones of the lens. (c) Cross section of the region marked in (b) reveals a local misalignment of 19 nm corresponding with 26.9 nm global misalignment along the diagonal. (e) Fourier components of the selected area imply 50.4% local diffraction efficiency among the smallest zones.

x-ray optics without increasing the complexity of the experimental setup by exchanging mechanical stacking to a monolithic, inherently stable setup. The produced blazed double-sided zone plates with 200 nm smallest zone width offer focusing efficiencies up to 54.7%. Moreover, our studies have shown that the alignment procedure can routinely provide alignment accuracy on the order of 30 nm. This would be sufficient for zone plates with sub-100 nm half-pitch, allowing the fabrication of both conventional and blazed double-sided zone plates for the multi-keV, x-ray range. We believe that the high-focusing efficiency, compact size, and stability provided by double-sided zone plates makes them excellent candidates for high-flux micro-diffraction and coherent diffractive imaging experiments.

**Funding.** Seventh Framework Programme (FP7) (290605, PSI-FELLOW/COFOUND).

**Acknowledgment.** The authors are grateful to A. Diaz for her help during the measurements. This project was carried out as a joint effort between the Paul Scherrer Institut (PSI) and the Nanoscopium beamline of the Synchrotron SOLEIL. The x-ray experiments shown here were performed at the cSAXS beamline at the Swiss Light Source, PSI, Villigen, Switzerland. Preliminary research was carried out at the light source PETRA III at DESY, Hamburg, a member of the Helmholtz Association (HGF). We thank Alke Meents and Karolina Stachnik for their assistance in using beamline P11. The research leading to these results has received funding from the European Union's Seventh Framework Programme (FP7/2007-2011) under grant agreement no. 290605 (PSI-FELLOW/COFOUND).

## REFERENCES

1. B. Kaulich, P. Thibault, A. Gianoncelli, and M. Kiskinova, J. Phys. **23**, 083002 (2011).
2. A. G. Michette, Rep. Prog. Phys. **51**, 1525 (1988).
3. J. L. Soret, Arch. Sci. Phys. Nat. **52**, 320 (1875).
4. J. Kirz, J. Opt. Soc. Am. **64**, 301 (1974).
5. E. DiFabrizio, F. Romanato, M. Gentili, S. Cabrini, B. Kaulich, J. Susini, and R. Barrett, Nature **401**, 895 (1999).
6. S. Tamura, M. Yasumoto, N. Kamijo, Y. Suzuki, M. Awaji, A. Takeuchi, K. Uesugi, Y. Terada, and H. Takano, Vacuum **80**, 823 (2006).
7. J. Maser, B. Lai, W. Yun, S. D. Shastri, Z. Cai, W. Rodrigues, S. Xua, and E. Trackhtenberg, Proc. SPIE **4783**, 74 (2002).
8. I. Snigireva, A. Snigirev, V. Kohn, V. Yunkin, M. Grigoriev, S. Kuznetsov, G. Vaughan, and M. DiMichiel, Phys. Status Solidi A **204**, 2817 (2007).
9. Y. Feng, M. Feser, A. Lyon, S. Rishton, X. Zeng, S. Chen, S. Sassolini, and W. Yun, J. Vac. Sci. Technol. B **25**, 2004 (2007).
10. I. Mohacsi, I. Vartiainen, M. Guizar-Sicairos, P. Karvinen, V. A. Guzenko, E. Müller, E. Färm, M. Ritala, C. M. Kewish, A. Somogyi, and C. David, Opt. Express **23**, 776 (2015).
11. S. Chen, A. Lyon, J. Kirz, S. Seshadri, Y. Feng, M. Feser, S. Sassolini, F. Duewer, X. Zeng, and C. Huang, Proc. SPIE **7448**, 74480D (2009).
12. I. Mohacsi, P. Karvinen, I. Vartiainen, V. A. Guzenko, A. Somogyi, C. M. Kewish, P. Mercére, and C. David, J. Synchrotron Radiat. **21**, 497 (2014).
13. A. G. Michette, *Optical Systems for Soft X Rays* (Plenum, 1986).
14. J. V.-C. S. Gorelick, V. A. Guzenko, and C. David, Nanotechnology **21**, 295303 (2010).
15. J. Vila-Comamala, M. Wojcik, A. Diaz, M. Guizar-Sicairos, C. M. Kewish, S. Wang, and C. David, J. Synchrotron Radiat. **20**, 397 (2013).
16. S. K. Dew and M. Stepanova, *Nanofabrication* (Springer Verlag, 2012).
17. Y. Shazia, D. G. Hasko, and H. Ahmed, Microelectron. Eng. **61–62**, 745 (2002).
18. M. Lindblom, H. M. Hertz, and A. Holmberg, J. Vac. Sci. Technol. B **24**, 2848 (2006).
19. B. Henrich, A. Bergamaschi, C. Broennimann, R. Dinapoli, E. F. Eikenberry, I. Johnson, M. Kobas, P. Kraft, A. Mozzanica, and B. Schmitt, Nucl. Instrum. Methods Phys. Res., Sect. A **607**, 247 (2009).
20. P. Thibault, M. Dierolf, A. Menzel, O. Bunk, C. David, and F. Pfeiffer, Science **321**, 379 (2008).
21. J. M. Rodenburg, A. C. Hurst, A. G. Cullis, B. R. Dobson, F. Pfeiffer, O. Bunk, C. David, K. Jefimovs, and I. Johnson, Phys. Rev. Lett. **98**, 034801 (2007).
22. M. Guizar-Sicairos, I. Johnson, A. Diaz, M. Holler, P. Karvinen, H.-C. Stadler, R. Dinapoli, O. Bunk, and A. Menzel, Opt. Express **22**, 14859 (2014).